

# Color digitizing and modeling of free-form 3D objects

Timothée Jost\*, Christian Schütz, Heinz Hügli

Institute of Microtechnology, University of Neuchâtel,  
CH-2000 Neuchâtel, Switzerland

## ABSTRACT

This paper deals with the problem of capturing the color information of physical 3D objects thanks to a class of digitizers providing color and range data, like range finders based on structured lighting. It appears typically in a modeling procedure that aims at building a realistic virtual 3D model. The color data delivered by such scanners basically express the reflected color intensity of the object and not its intrinsic color. A consequence is therefore the existence, on the reconstructed model, of strong color discontinuities, which result from acquisitions done under different illumination conditions. The paper considers three approaches in order to remove these discontinuities and obtain the desired intrinsic color data. The first one converts the reflected color intensity into the intrinsic color by computation, using a reflectance model and known acquisition parameters. The use of simple reflectance models is considered: Lambert and Phong, respectively for perfectly diffuse and mixed diffuse and specular reflection. The second approach is a hardware solution. It aims at using a nearly constant, diffuse and omnidirectional illumination over the visible parts of the object. A third method combines the first computational approach with the use of several known illumination sources. An experimental comparison of these three approaches is finally presented.

**Keywords:** range image, reflectance model, color digitizing, 3D object modeling

## 1. INTRODUCTION

3D object modeling methods have been presented in a lot of papers these last years and many applications are concerned with virtual 3D models. The range extends from industrial inspection to rapid prototyping and from special effects in movies to virtual museum. These days, 3D scanners tend to be used more and more since the model construction with a standard CAD tool or a manual pointing device is quite a tedious task, especially for free-form objects.

As objects self occlude, a 3D scanner can only capture a part of their surface at one time. Building a full model requires the combination of several views of the object. Automatic or semi-automatic merging of a set of range views into a complete geometrical model has been much investigated for the past decade.

Beside geometry, color data is essential to create a realistic model of an object: 3D models won't look realistic if only their geometrical aspect is taken into account; the appearance of an object is also important. Realistic appearance is obtained by assigning either a color or a subimage to each model mesh, respectively leading to a colored or a texture-mapped object model.

This paper focuses on the problem of capturing the color information of physical 3D objects thanks to range finders based on structured lighting. This kind of scanner permits an easy measurement of both color and geometric information since it mainly uses a CCD camera and a projector to retrieve range data. In addition, the color picture of the object that is provided by the camera is in perfect registration with the range image. Unfortunately, the color components delivered by these scanners express the reflected color intensity of the object and not its intrinsic color as required for the object model. A consequence of this is therefore the existence on the reconstructed model of strong color discontinuities, which appear on the boundaries of two object views because their acquisition was done under different illumination conditions.

Light reflection has been studied specifically in the field of computer graphics. Ikeuchi and Sato<sup>3</sup> proposed a method to compute the reflectance parameters of objects from range and intensity data. Their work however assumes that the object consists all of the same material and considers one set of parameters for the whole object. Baribeau *et al.*<sup>1</sup> present a reflectance model used to characterize the intrinsic color properties of objects measured with a polychromatic laser range

---

\* Correspondence: Email: timothee.jost@imt.unine.ch; WWW: <http://www-imt.unine.ch>; Telephone: +41 32 7183459;  
Fax: +41 32 7183402

sensor. Kay and Caelli<sup>5</sup> proposed recovering reflectance parameters for every point of an object, considering a range and several intensity images. They use a modified version of the Torrance-Sparrow model. Compared with others, the present work is less concerned with quantitatively exact color but concentrates on obtaining the qualitatively correct texture of the object, using a very simple and basic model, and mainly cares about the good appearance of the resulting color image.

Two main reflectance types can be observed on a physical object: diffuse and specular. To account for it, this work successively considers the Lambertian and then the Phong model<sup>2</sup>. Three different approaches will be considered to obtain the desired intrinsic color.

The first one converts the reflected color intensity into the intrinsic color by computation. It operates with the projector of the range finder as only light source, and uses therefore the color image as provided by the video camera of the 3D scanner. In order to compensate for varying light illumination, it uses a reflectance model and operates then on known illumination, camera and surface orientations to compute the compensation.

The second approach aims at using a nearly constant, diffuse and omnidirectional illumination over the visible parts of the object. It is a hardware solution. Creating such a uniform diffuse illumination around the object can be done with several white light sources that must be distributed as homogeneously as possible.

A third method proceeds according to the first approach but tries additionally to get rid of specularities by using several known illumination sources.

Section 2 exposes the working principle of the structured light range finder and section 3 presents an overview of color object modeling from range images in general. The different methods to obtain the intrinsic color model are explained in the next section. A last section is devoted to a number of experiments, conducted in order to assess the feasibility of these methods.

## **2. STRUCTURED LIGHT RANGE FINDERS**

Several types of 3D scanners (or range finders) can be found on the market today. Most of these devices are based on vision, which offers the advantage of having no physical contact with the measured object. These tools measure the spatial position of points on a surface and usually provide the result as a range image, the value of each pixel being the point to scanner distance. One can mainly distinguish four measurement techniques: passive triangulation, active triangulation, laser radar and focus:

- Passive triangulation, or stereo vision, uses at least two different views of the scene. Low level features are then directly matched. Range information can be obtained, knowing the relative position and orientation of each camera.
- In active triangulation, a light spot, line or grid is projected on the object and observed from a different angle, by a CCD camera. Range data can be computed by triangulation.
- For laser radar, a laser beam is directed on the object and data is calculated thanks to time of flight or phase shift measurements.
- Finally, the focus technique determines the range value of a point, considering the lens configuration that gives the best focus for this point.

In this paper, we will concentrate on structured light range finders. These scanners are based on the active triangulation technique and use the principle of the line projection method: a sheet of light (usually created with a laser passing through a cylindrical lens) intersects a reference plane. The corresponding line is observed with a CCD camera, whose position is different from the source of the light sheet. If no object is present, one can observe a straight line (fig.1. a). If an object is put in front of the sheet of light, the line will be distorted (fig. 1. b). A calibrated system permits the computation of range values on this line. To scan the whole object, one needs to perform a mechanical translation of either the object or the sensor.

In a structured light range finder, the line projector is replaced with a pattern projector. It works on the principle of space coding. It covers the whole area of interest with several black and white stripe patterns of different size. Each light sheet is now represented with its own unique binary code (fig. 2.). The advantage of this technique is that there is no need to move the sensor to cover the whole object. Another advantage is that color digitizing is very simple with such a scanner. One just has to take a color picture with the camera. This color image is in perfect registration with the range image (fig. 3.) and possesses the same sampling rate, due to the fact that there is no translation of either object or sensor. There is no need to perform data fusion from two independent sensors.

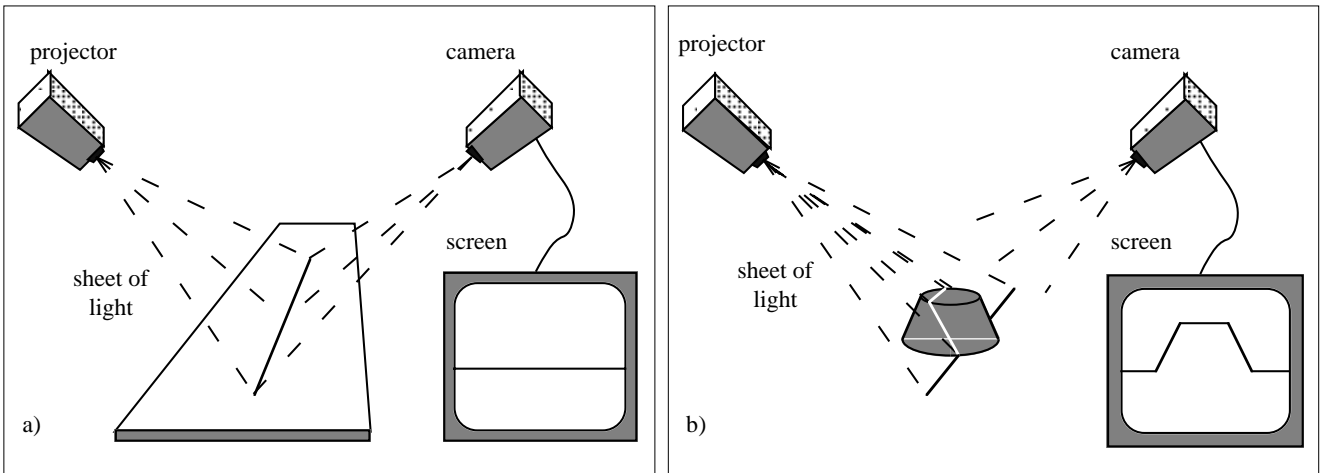


Figure 1. Line projection range finder principle. (a) A reference plane is present, the intersecting line is straight. (b) The object creates a distortion of the line.

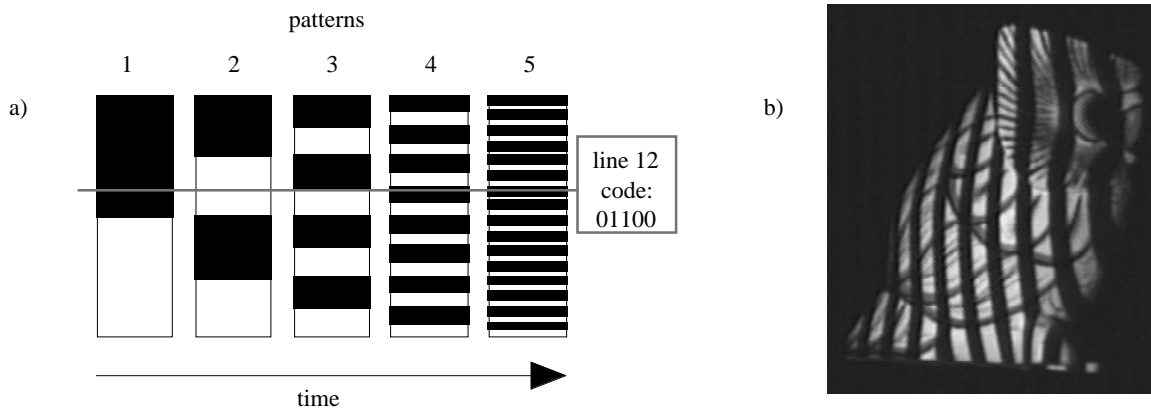


Figure 2. Projected patterns for space coding. (a) Example with 5 patterns. (b) Example of patterns projected on object owl.

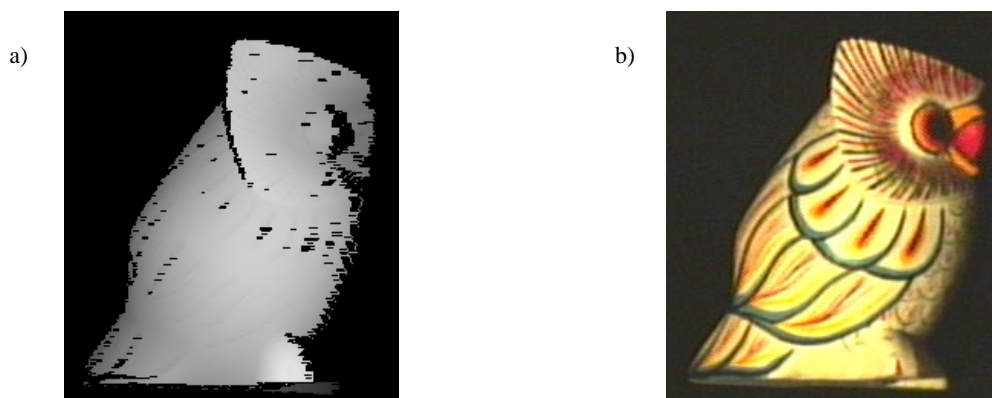


Figure 3. (a) Range image. (b) Color image

If structured light range finders have good advantages as mentioned above, they also pose some problems. The first one is that any acquisition has to be done in the dark. Then, the object can create shadows on itself. These shadowed surfaces can't be measured, because of the absence of pattern. Finally, the same problem may arise when the object contains very dark colors: projected patterns just have too low a contrast to be detected.

### 3. COLOR OBJECT MODELING FROM RANGE IMAGES

The task of object modeling from range images mainly consists in merging a set of range views that collectively cover the whole surface of the object to be finally left with a unique surface. Data acquisition excepted, the process can be divided in two main parts: positioning and integration.

#### 3.1. Positioning

Positioning is the attempt to find the correct relative alignment of two or more views. This is straightforward if, during the acquisition process, the object is kept into a calibrated configuration, like on a turntable. However, in many cases, positioning is not performed during the acquisition and must be solved at a later stage. In that case, registration is necessary. It can be based on special marks which are to be brought onto the object. It can also be based on the object geometry itself, in which case registration involves the geometric matching of surfaces

#### 3.2. Integration

After registration, the views need to be integrated together, in order to be left with a unique surface representing the virtual object. A wide variety of methods are available, from keeping most of the original structure of the views to building a whole new surface from the cloud of points formed by the registered views. Whatever method is used, color problems, like discontinuities, may appear if one tries to mix colors that are not the same on different views.

#### 3.3. Registration Using Color

The case of the registration of views thanks to geometric matching of surfaces is presented in<sup>6</sup>. Central to the geometric matching is the iterative closest point (ICP) algorithm. Schütz *et al.*<sup>6</sup> expose the usefulness of adding color and surface orientation parameters to this algorithm. This can be taken as another motivation for intrinsic color recovery.

#### 3.4. Texture Extension

The objects we are referring to in this work are modeled by using a method presented by Jost *et al.*<sup>4</sup>. It proposes a reconstruction method that applies to textured views: each view is a triangle mesh built considering a sub sampling of the range image and the texture is created by mapping the color image on this 3D mesh.

The principle of the integration step is to remove the overlapping part of one of the views, namely P, and to fill the resulting gap between P and the other surface, X, with new triangles, keeping most of the original triangulation. To reduce the discontinuities that appear along the boundaries between textures from both surfaces, the texture image of P is iteratively extended on X, replacing the original texture of X with the redundant texture of P. This is named texture extension and is done as long as the resolution of texture P is better.

Finally, to insure a smooth color transition, a filtering of the triangles of the boundaries is performed, by applying a weighted averaging of both textures.

## 4. INTRINSIC COLOR RECOVERY METHODS

When looking at an object (with eyes, camera, etc...), the sensed colors or intensities depend on the object and on its illumination as well. Several illumination factors have an influence: number and position of light sources, their orientation or their spectrum. This means that the sensed color of the same point of an object will generally not be the same under different illumination conditions. Of course, this is also the case with the color image of the range sensor: when the object is moved for another view, the relative illumination changes and different sensed colors will characterize the same object point in different view. A way to convert the sensed colors in the intrinsic object color is required to solve this problem.

Generally, the light interaction at the surface of the object results from several physical phenomenon. The reflected light depends on incident light and the most general description of the geometrical relations is given by the bi-directional reflection distribution function<sup>7</sup> (BRDF). Measuring the BRDF of a given surface is tedious because it is a function of four variables. Simple models of light reflection are therefore used in the computer graphics domain.

This section describes the different methods we used to recover the intrinsic color of objects scanned with a structured light range finder. The first method tries to retrieve the color information of an object, using the projector as the only source of illumination. Thus, this method is characteristic of the structured light range finder. The second and third methods use external light sources and can therefore be possibly applied to other scanning techniques: active, passive or focus.

#### 4.1. Reflectance Model

The reflectance model in use here is one among the computer graphics models, the Phong model<sup>2</sup>. It is a simple approximation of the light reflection phenomenon, which can be partly explained by the following: when light strikes the surface of an object, a part of it is reflected and the other part just penetrates the matter. The reflected light percentage is referred to as specularity and it "bounces" off in a precise direction determined by the angle of incident light and the orientation of the surface. Practically, depending on the surface roughness, the reflected light can be more or less spread around the specular direction. A part of the penetrating light is definitely absorbed by the matter but the rest is randomly re-emitted. This absorption / emission process is called diffusion.

In the early 60's, Lambert proposed a very simple and intuitive model for diffusion<sup>2</sup>. It considers a constant diffuse reflection of a surface point in every direction. For a single light source, along direction  $\mathbf{S}$ , the radiance is given by

$$L(\mathbf{V}) = L = k_d L_s (\mathbf{S} \cdot \mathbf{N}) = k_d L_s \cos \theta \quad (1)$$

where  $L_s$  is the radiance of an ideally white surface oriented towards the light source,  $k_d$  is a constant depending on the object material,  $\mathbf{N}$  is the surface orientation (normal) and  $\theta$  is the angle between  $\mathbf{S}$  and  $\mathbf{N}$  (fig. 4., every vector has a norm of 1).

We can easily recover  $k_d$  from (1)

$$k_d = \frac{L}{L_s \cos \theta}$$

$k_d$  is the reflection coefficient of the surface. In the perfect case, it's value ranges from 0 for black to 1 for white. It is the expected intrinsic object feature.

In the mid 70's, Phong proposed a model that also takes ambient light and specularity into account. It uses an exponentiated cosine to model the specular highlights:

$$L(\mathbf{V}) = k_a L_a + k_d L_s (\mathbf{S} \cdot \mathbf{N}) + k_s L_s (\mathbf{R} \cdot \mathbf{V})^{k_e} = k_a L_a + k_d L_s \cos \theta + k_s L_s (\cos \alpha)^{k_e} \quad (2)$$

where  $k_s$  is a scalar constant,  $k_e$  is called roughness or shininess exponent and  $\mathbf{R}$  is the specular reflection direction (fig. 4.), given by the simple relation

$$\mathbf{R} = \mathbf{S} + 2(\mathbf{S} \cdot \mathbf{N})\mathbf{N}$$

$k_a L_a$  is called ambient light. It takes indirect light effects into account. Indirect lightning is the result of reflection or transmission of light on other objects, walls etc... that indirectly illuminates the considered object. Of course, this is a very simple approximation because it considers indirect lighting as constant everywhere, but we will see later that it has some practical importance.

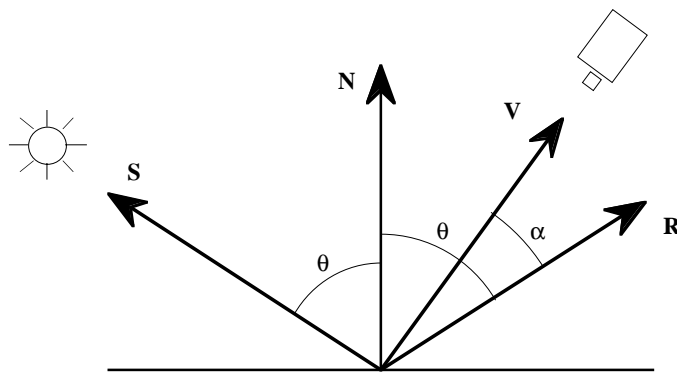


Figure 4. Vectors used for the reflectance model.

#### 4.2. First Method: Single Light Compensation

This method considers the object illuminated by a single source of light, which is the projector of the structured light range finder. The goal is to invert the reflectance model in order to compensate for varying light illumination. Illumination and camera position are known from the calibration process and surface orientations can be computed from the range data.

Considering the Phong model (2), the problem is that, generally, it can't be inverted near the specular direction. Practically, the specular component is so intense near that direction that the image is saturated, leaving no information about the intrinsic color of the object. Thus, for this model, we will keep only the diffuse and ambient component. This gives the relation:

$$k_d = \frac{L/L_s - k_a L_a/L_s}{\cos \theta} \quad (3)$$

To measure the incoming light, we use a CCD camera and a frame grabber. The video signal is converted into a digital red, green and blue (r,g,b) signal to create the color image. In our case, the radiance is proportional to the color vector and, consequently, we will use (3) on each component of the  $\mathbf{C} = (r, g, b)$  vector:

$$\mathbf{C}_d = \frac{\mathbf{C} - \mathbf{C}_a}{\cos \theta} \quad (4)$$

where  $\mathbf{C}$  is a pixel of the color image and  $\mathbf{C}_a$  is the ambient component.

One can note that the image acquisition device often delivers a signal that is affected by some offset value. The ambient term can also be used to compensate for this unwanted offset.

#### 4.3. Second Method: Constant Illumination

Instead of trying to use one known light source and convert the reflected color intensity back into intrinsic color, the second approach aims at using a nearly constant, diffuse and omnidirectional illumination over the visible parts of the object. Theoretically, the goal is to create an infinite number of very small light sources that illuminate each visible face of the object from every direction. Practically, creating such a uniform diffuse illumination around the object can be done with several white light sources that must be distributed as homogeneously as possible.

#### 4.4. Third Method: Multiple Light Compensation

The first method does not permit to measure the color of the object in case of important specular reflection. In order to overcome this problem, the idea is to apply the same theory to several light source positions and orientations: the data now consist of one range image and several color images, taken while using different positions of the light source. The resulting image is computed by weighted averaging of each compensated input images.

The present method uses the Phong model. The goal here is to consider one color image per light source position. Each of these images is modeled by

$$L_i(\mathbf{V}) = k_a L_a + k_d L_i (\mathbf{S}_i \cdot \mathbf{N}) + k_s L_i (\mathbf{R}_i \cdot \mathbf{V})^{k_e} = k_a L_a + k_d L_i \cos \theta_i + k_s L_i (\cos \alpha_i)^{k_e}$$

Because the *same light sources* are used at approximately the *same distance*, the radiance of each source is constant:  $L_i = L_s, \forall i$ . To simplify the relation, from now on, we will consider offset compensated and normalized images:  $L'_i(\mathbf{V})$ . Considering diffusion, for each image  $i$ , we then have

$$L'_i(\mathbf{V}) = \frac{L_i(\mathbf{V})}{L_s} - \frac{k_a L_a}{L_s} \Rightarrow k_d^i = \frac{L'_i}{\cos \theta_i}, \forall i$$

and the weighted average  $k_d$  for  $n$  sources is:

$$\bar{k}_d = \frac{\sum_{i=0}^{n-1} w_i k_d^i}{\sum_{i=0}^{n-1} w_i} = \frac{\sum_{i=0}^{n-1} w_i L'_i / \cos \theta_i}{\sum_{i=0}^{n-1} w_i} \quad (5)$$

A sensitivity analysis shows that the error (uncertainty) on  $k_d$  increases when  $\cos\theta$  gets smaller, i.e. when  $\theta$ , the angle of incidence of the light, increases. Therefore, a good idea is to choose weights  $w_i$  that decrease for higher values of  $\theta$ . Simply choosing  $w_i = \cos\theta_i$ , (5) now becomes:

$$\bar{k}_d = \frac{\sum_{i=0}^{n-1} L'_i}{\sum_{i=0}^{n-1} \cos\theta_i}$$

Finally, the fact that there exist color images from different illuminations is used to eliminate specularity. The factors  $w_i$  must be modified to depend on specularity. To get rid of the specular pixels in a particular image,  $w_i$  must be smaller near the specular axis:

$$\begin{aligned} \text{if } (\cos\alpha_i)^{k_e} \rightarrow 0 &\Rightarrow w_i \rightarrow \cos\theta_i \quad (\text{diffusion}) \\ \text{if } (\cos\alpha_i)^{k_e} \rightarrow 1 &\Rightarrow w_i \rightarrow 0 \quad (\text{specularity}) \end{aligned}$$

taking  $w_i = \cos\theta_i \left(1 - (\cos\alpha_i)^{k_e}\right)^{k_o}$ , (5) then becomes

$$\bar{k}_d = \frac{\sum_{i=0}^{n-1} \left(1 - (\cos\alpha_i)^{k_e}\right)^{k_o} L'_i}{\sum_{i=0}^{n-1} \cos\theta_i \left(1 - (\cos\alpha_i)^{k_e}\right)^{k_o}}$$

Considering the (r,g,b) color components of the color images, the compensation transform is:

$$\bar{\mathbf{C}}_d = \frac{\sum_{i=0}^{n-1} \left(1 - (\cos\alpha_i)^{k_e}\right)^{k_o} (\mathbf{C}_i - \mathbf{C}_a)}{\sum_{i=0}^{n-1} \cos\theta_i \left(1 - (\cos\alpha_i)^{k_e}\right)^{k_o}} \quad (6)$$

where  $\mathbf{C}_i$  is a pixel of the color image  $i$  and  $\mathbf{C}_a$  is the ambient component.

## 5. EXPERIMENTS AND RESULTS

The following section presents experiments conducted in order to validate and compare the different methods. All these investigations were done with an experimental modeling software and hardware. Some features are as follow. The 3D scanner consists of a JVC color CCD camera (VC 4913) and an ABW LCD-320 projector. This projector can cast up to 320 lines, giving a 512x512 range image with a maximal resolution of about 0.5mm for objects of typical size between 50 and 200 mm. The modeling software works on a SGI Indigo2 impact workstation and is programmed with the Open Inventor library in C++.

The optimal omnidirectional illumination consists of four large reproduction lights and diffusing paper. Arrangement and distance are selected to obtain the best possible uniform illumination. The same lights, but without diffuser, are used as directional light to test the multiple lights compensation method.

### 5.1. Measure of Indirect Lighting

The measurement of ambient light is performed with a setup where a white sphere is illuminated by a single directional light source. Both the dark side of the sphere and the non-illuminated black background are measured. The results are found in table 1 (range 0-255, r channel, r,g,b have approx. the same distribution).

Table 1. Measure of indirect lighting and offset.

	mean value	standard deviation
dark side of sphere	55	3.0
black image	51	2.4

Looking at the difference between a black image and indirect light on sphere, one can conclude that the indirect light influence is very low (1.5-2%) but that there is an important offset (15-20%) on black value, coming from the acquisition system. This effect is not due to indirect light but we will consider it as such. A value for  $\mathbf{C}_a = (C_a, C_a, C_a)$  was chosen accordingly.

### 5.2. Comparison of the Methods Regarding Diffusion

This is a practical comparison of the three methods in the context of object modeling. The task consists in the modeling of a mainly diffuse, painted wooden owl (fig 5. a), using the different methods. 8 views were used to create the full models. Each model contains approximately 5000 points and 10000 faces. The modeling was performed using the textured views approach exposed in section 3 and two models were built for each intrinsic color recovery method. The first case is without texture extension. It permits to compare texture near the border of the views, where the angle between the normal of the surface and the view direction is high, creating a bigger uncertainty on geometry and color. The second model was built using texture extension. In both cases, filtering of the texture boundaries was not applied to let them be apparent. Figure 5 presents a typical texture frontier as it appears on models reconstructed with and without texture extension for each method. A rendered picture of the model can be seen in (a). (b) exposes close-ups of a texture boundary. The texture images were obtained using the projector as only illumination source. The discontinuities can easily be observed on the left picture. These discontinuities are much less visible when using texture extension (right picture), the difference in the relative angle of illumination now being smaller between both side of the boundary. Close-ups of the same texture boundaries, obtained using each method, are presented in (c).

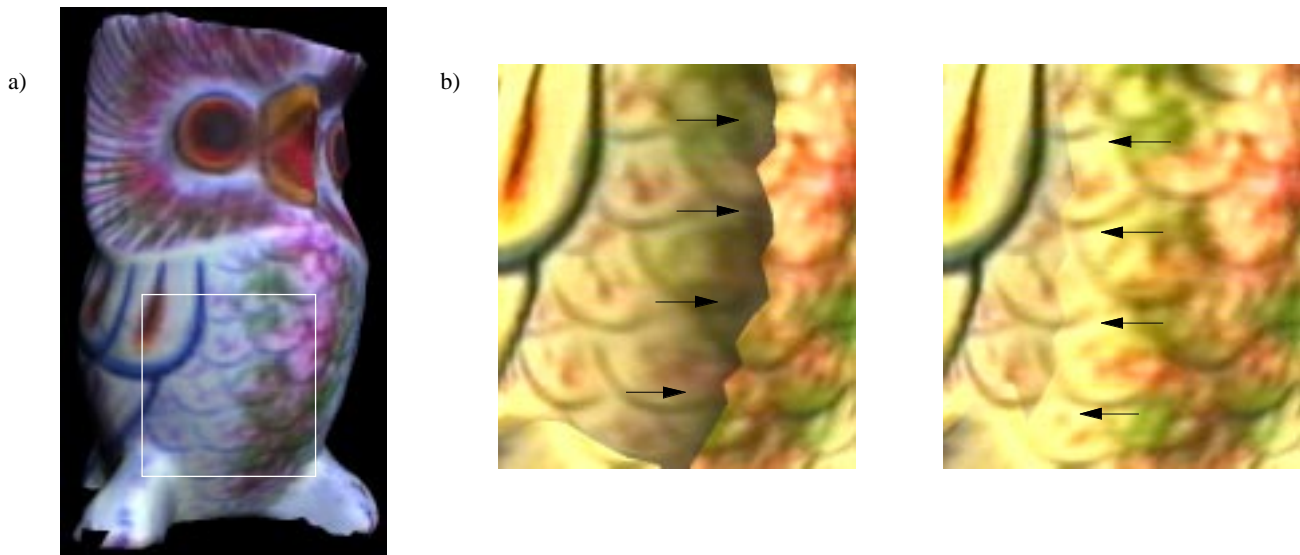


Figure 5. Comparison of the methods applied to object owl. (a) Rendered owl model. (b) Close-ups on a texture boundary; model created without using any compensation method; texture extension is used in the right picture.

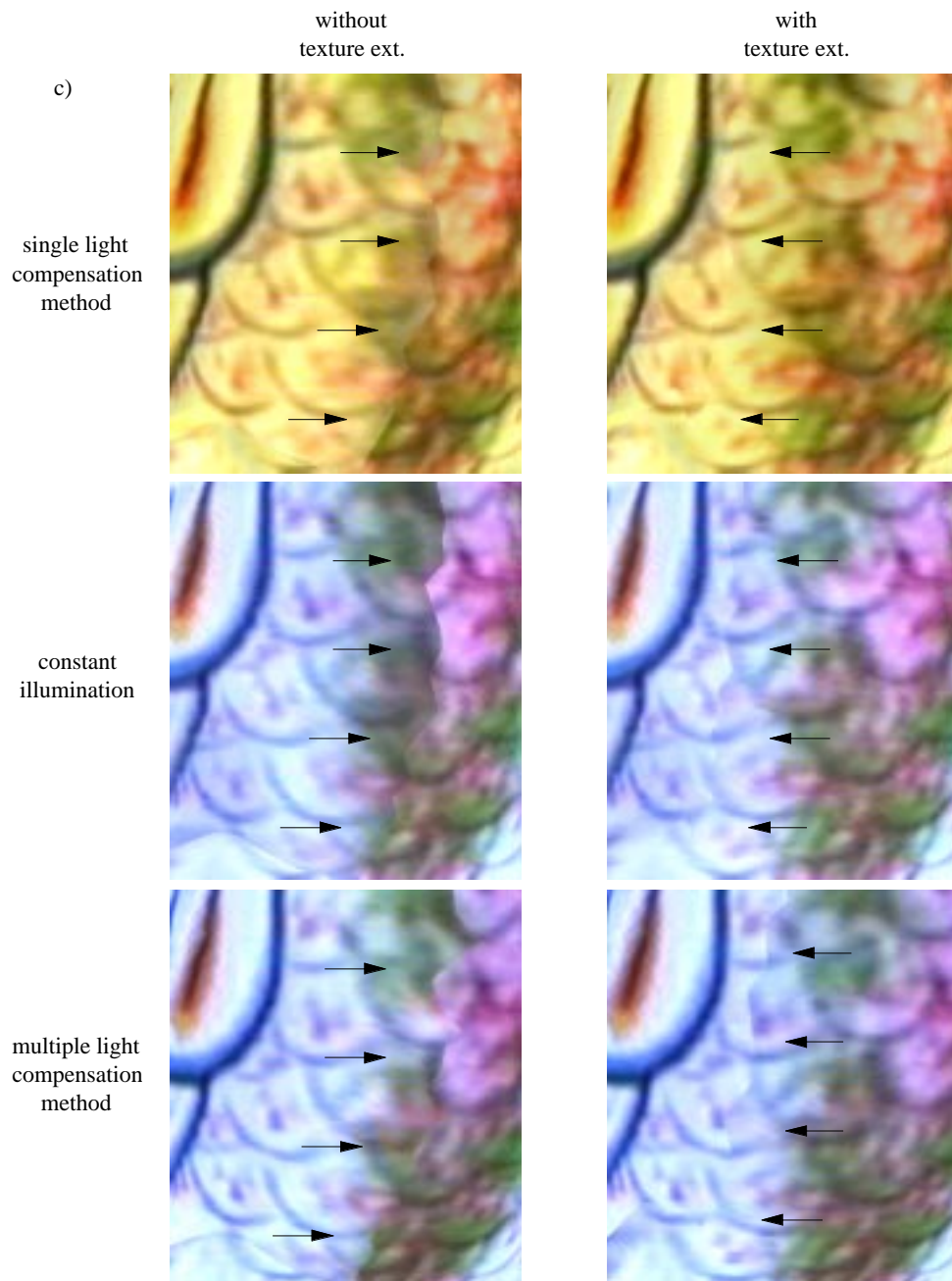


Figure 5. (c) Close-ups on the same texture boundary, comparing the three compensation methods; texture extension is used in the right picture.

### 5.3. Comparison of the Methods Regarding Specularity

This is a comparison of the three methods for a highly specular object, a metallic can of paint spray. Each method was applied to the same view of the spray. Figure 6 presents the results in the form of the texture map. As expected, the first two methods keep the specular reflection in the image. The second method reduces them (in fact it increases the diffusion) but with very specular objects, the result can be even worse than in the first method, creating several reflections. The multiple light compensation method shows to be useful here, the specular reflections being nearly invisible.

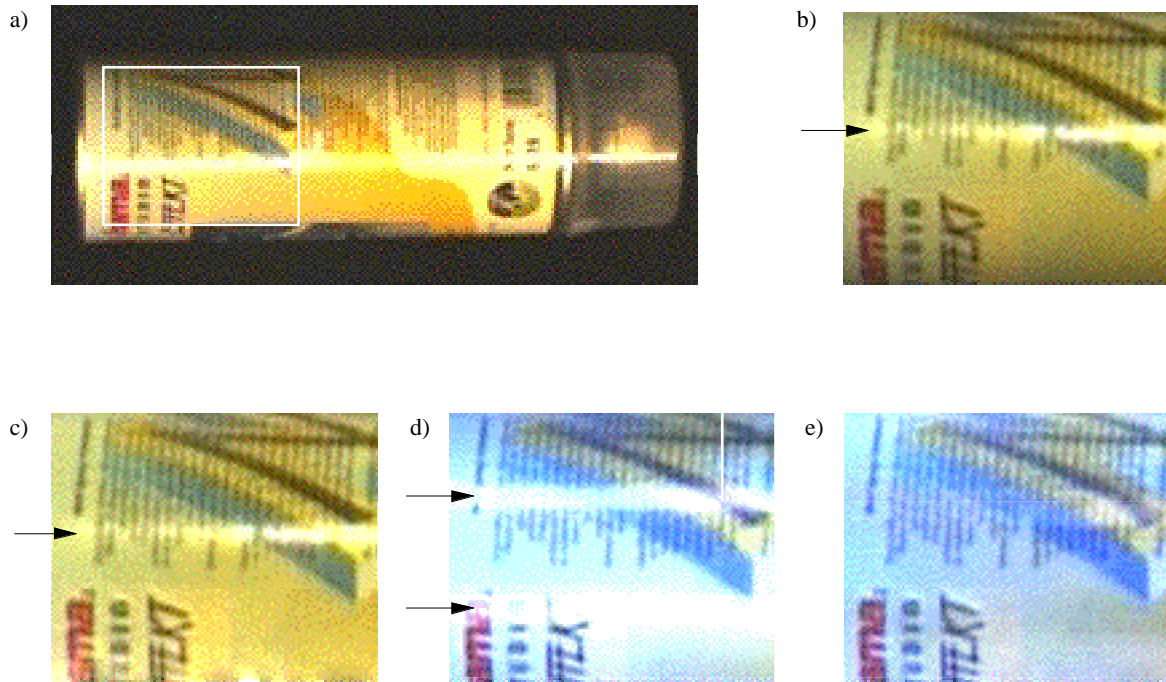


Figure 6. Comparison of the methods applied to object spray.

### 5.4. ICP Coupling Test

This test is meant to illustrate the usefulness of color compensation in the case of the registration process using color, for object recognition or modeling for example. A pair of views that have an overlap of about 50% is considered here. The color map of those views was scanned using the different compensation methods. Both views are first registered to reach their optimal position and then, the coupling percentage of the registration (points that are subject to be compatible) is measured, considering colors, with and without compensation. Table 2 gives the percentage of points that were coupled for two different pairs.

Table 2. Comparison of methods considering the ICP coupling percentage.

	no compensation	1st method	2nd method	3rd method
first pair	33	43	42	43
second pair	27	43	39	-

The difference between compensation and no compensation is visible: about 35% more points can be matched after color compensation. This result shows how illumination effects can degrade the matching quality. The coupling is approximately the same for every compensation methods.

## 5.5. Discussion

The first method uses the sole range scanner; it has the advantage of not requiring additional hardware. Highly reflective objects can pose a problem, because specularities aren't considered in the final model. Furthermore, colors near the boundary of the views (important angle between light axis and surface normal) tend to have a higher uncertainty.

The second and third methods require additional hardware, namely external sources of light. Trying to create a constant illumination seems to be hard to achieve with a basic lighting material. Although the results are not bad, the comparison with the other two methods shows inferior quality in terms of diffusion. For object of low specularity, this method provides better results than the single light compensation method but the results are bad with highly specular objects.

The third method shows to be effective in presence of specular reflections. It also reduces the effects of the boundary problem found with the first method. Some limitations remain: the parameters need to be changed manually for different objects and consequently are not optimal. This method is also limited to convex objects; for the moment, the shadows an object creates on itself are not taken into account.

## 6. CONCLUSION

Many applications require realistic color virtual models. This paper presents and discusses three simple methods that can be used in order to recover the intrinsic colors of an object captured with a structured light range finder. The first one uses the projector as unique light source and converts the reflected color intensity into the intrinsic color by computation, using a reflectance model and known acquisition parameters. The second approach is a hardware solution: it aims at using a nearly constant, diffuse and omnidirectional illumination over the visible parts of the object. A third method combines the first computational approach with the use of several known illumination sources.

The results confirm that these methods can be successfully applied to a number of objects. The experiments show that the first simple method only applies in presence of diffusing objects. In presence of specular objects, the third method is recommended.

## REFERENCES

1. R. Baribeau, M. Rioux, G. Godin, "Color Reflectance Modeling Using a Polychromatic Laser Range Sensor", *Pattern Analysis and Machine Intelligence*, vol. 14, no. 2, pp. 263-266, 1992.
2. Andrew S. Glassner, *Principles of Digital Image Synthesis*, vol. 2, ch. 13, 15, Morgan Kaufmann Publishers Inc., San Francisco, 1995.
3. K. Ikeuchi, K. Sato, "Determining Reflectance Parameters using Range and Brightness Images", *Pattern Analysis and Machine Intelligence*, vol. 13, no. 11, pp. 1139-1153, 1991.
4. T. Jost, C. Schütz, H. Hügli, "Modeling 3D Textured Objects by Fusion of Multiple Views", *Signal Processing IX, Eusipco 98*, vol. 2, pp. 1073-1076, Typorama Publications, Rhodes, 1998.
5. Greg Kay, Terry Caelli, "Inverting an Illumination Model from Range and Intensity Maps", *CVGIP: Image Understanding*, vol. 59, no. 2, pp. 183-201, 1994.
6. C. Schütz, T. Jost, H. Hügli, "Multi-Feature Matching Algorithm for Free-Form 3D Surface Registration", *14th International Conference on Pattern Recognition, ICPR'98*, vol. 2, pp. 982-984, IEEE Computer Society, Brisbane, 1998.
7. Eaton, F. D., I. Dirmhin, "Reflected Irradiance Indicatrices of Natural Surfaces and their Effect on Albedo", *Applied Optics*, vol. 18, no. 7, pp. 994-1008, 1979.